Received: 30 June 2020 | Revised: 21 August 2020 | Accepted: 26 August 2020 | Published online: 25 September 2020

DOI: 10.1002/dad2.12109

Alzheimer's & Dementia
Diagnosis, Assessment & Disease Monitoring

RESEARCH ARTICLE

Sectoral segmentation of retinal amyloid imaging in subjects with cognitive decline

Oana M. Dumitrascu[1] | Patrick D. Lyden[1] | Tania Torbati[2] | Julia Sheyn[2] | Ayesha Sherzai[3] | Dean Sherzai[3] | Dale S. Sherman[4] | Ryan Rosenberry[5] | Susan Cheng[5] | Kenneth O. Johnson[6] | Alan D. Czeszynski[6] | Steven Verdooner[6] | Sally Frautschy[7] | Keith L. Black[2] | Yosef Koronyo[2] | Maya Koronyo-Hamaoui[2,8]

[1] Department of Neurology, Cedars-Sinai Medical Center, Los Angeles, California, USA

[2] Department of Neurosurgery, Cedars-Sinai Medical Center, Los Angeles, California, USA

[3] Department of Neurology, Loma Linda University, Loma Linda, California, USA

[4] Department of Neuropsychology, Cedars-Sinai Medical Center, Los Angeles, California, USA

[5] Department of Cardiology, Cedars-Sinai Medical Center, Los Angeles, California, USA

[6] NeuroVision Imaging Inc., Sacramento, California, USA

[7] Department of Neurology, University of California Los Angeles, Los Angeles, California, USA

[8] Biomedical Sciences, Cedars-Sinai Medical Center, Los Angeles, California, USA

Correspondence
Oana Dumitrascu, Cedars Sinai Medical Center, 127 S. San Vicente Blvd, A6302, Los Angeles, CA 90048, USA.
Email: dumitrascu.oana@mayo.edu
Maya Koronyo-Hamaoui, Cedars Sinai Medical Center, 127 S. San Vicente Blvd, A6212, Los Angeles, CA 90048, USA.
Email: Maya.koronyo@csmc.edu

Funding information
National Institute on Aging; National Institutes of Health, Grant/Award Numbers: R01 AG055865, R01 AG056478; The Saban and Gordon Private Foundations

Abstract

Introduction: Despite advances in imaging retinal amyloidosis, a quantitative and topographical investigation of retinal amyloid beta burden in patients with cognitive decline has never been reported.

Methods: We used the specific amyloid-binding fluorophore curcumin and laser ophthalmoscopy to assess retinal amyloid imaging (RAI) in 34 patients with cognitive decline. We automatically quantified retinal amyloid count (RAC) and area in the superotemporal retinal sub-regions and performed correlation analyses with cognitive and brain volumetric parameters.

Results: RAC significantly and inversely correlated with hippocampal volume (HV; r = -0.39, $P = .04$). The proximal mid-periphery (PMP) RAC and RA areas were significantly greater in patients with Montreal Cognitive Assessment (MOCA) score < 26 ($P = .01$; Cohen d = 0.83 and 0.81, respectively). PMP showed significantly more RAC and area in subjects with amnestic mild cognitive impairment (MCI) and Alzheimer's disease (AD) compared to cognitively normal ($P = .04$; Cohen d = 0.83).

Conclusion: Quantitative RAI is a feasible technique and PMP RAC may predict HV. Future larger studies should determine RAI's potential as a biomarker of early AD.

KEYWORDS
Alzheimer's disease, amyloid beta, brain volumetric analysis, confocal scanning ophthalmoscope, neurodegenerative disease, Retia, retina

1 | INTRODUCTION

Alzheimer's disease (AD) is a devastating neurodegenerative disorder and the most prevalent form of dementia, associated with enormous social and public health challenges.[1] Considerable evidence supports that quantitative imaging of biofluid biomarkers of AD pathology, amyloid beta (Aβ), tau, and neurodegeneration, may be useful predictors of subsequent cognitive decline.[2] Aβ is a pathological hallmark of AD, the target of disease-modifying therapies,[3] and useful in discriminating AD from other neuropathologies.[4] Surrogate markers of brain Aβ amyloidosis include reductions in $A\beta_{42}$ levels in the cerebrospinal fluid (CSF) and increased amyloid tracer retention on positron emission tomography (PET) imaging.[5,6]

Increased Aβ burden and Aβ deposits were also identified in the human AD retina, a central nervous system (CNS) tissue that has the advantage of increased accessibility for direct non-invasive visualization.[7–15] Clinical and preclinical data support that retinal Aβ deposition correlates with and may even precede cerebral Aβ deposition.[7,13,16–19] Modern technology was recently developed to image retinal amyloidosis in patients with AD,[13,20–22] as fluorescence signal and other retinal features may aid in predicting cerebral amyloid status.[17,23] One of the contemporary imaging modalities is curcumin-enhanced retinal fluorescence imaging that was pioneered as a useful non-invasive tool for retinal Aβ plaque detection in animals and humans.[7,9,13]

Curcumin has a chemical structure similar to that of Congo red and binds to the beta-pleated sheets in Aβ aggregates with high affinity and specificity.[24,25] In the tissue, curcumin displays natural fluorescence with peak excitation and emission wavelengths of 420 and 520 nm, respectively.[26] Curcumin is a safe product on the US Food and Drug Administration (FDA) Generally Recognize as Safe (GRAS) list, and can be used to enhance the intrinsic autofluorescence signal of Aβ.[24,25,27–29] We previously demonstrated the specificity of curcumin labeling of retinal Aβ deposits and its optical signature both ex vivo and in vivo.[7,13] In a proof-of-concept study, we showed the ability to image at high resolution and quantify retinal Aβ deposits and found significantly higher retinal amyloid burden in AD patients as compared to cognitively normal (CN) controls.[13] Prior studies have indicated that the superotemporal retinal region is especially affected in AD.[12,13,17,30] In order to develop a sensitive and specific imaging technique for widespread clinical and research use, it is critical to be able to determine the retinal subregions most predictive of cognitive loss.

In this cohort study, we aimed to investigate quantitative retinal amyloid imaging (RAI) in a population of patients with mostly amnestic mild cognitive impairment (aMCI), using a new modified iPAD-controlled ophthalmic device that is user- and patient-friendly. We introduced a new image-processing sectoral segmentation system for evaluating retinal amyloid burden in predefined topographic regions in the superotemporal quadrant. We further assessed the potential correlation of subregional retinal amyloid scores with demographic, cognitive, and brain imaging parameters.

HIGHLIGHTS

- Quantitative curcumin-enhanced retinal amyloid fluorescence imaging is feasible and non-invasive.
- Amyloid count in superotemporal retina is increased in mild cognitive impairment.
- Mid-peripheral retinal amyloid count inversely correlates with hippocampal volume.

RESEARCH IN CONTEXT

1. **Systematic review**: The authors reviewed the scientific literature and meeting abstracts. Retinal amyloid beta (Aβ) correlates with brain Aβ burden. Various imaging techniques were discovered to visualize retinal amyloidosis. As our group developed and translated curcumin-enhanced retinal fluorescence amyloid imaging in human trials with Alzheimer's disease (AD) patients, we sought to topographically and quantitatively investigate retinal amyloidosis in patients with mild cognitive impairment (MCI). Also for the first time, we sought to assess possible correlations between retinal amyloidosis, brain atrophy, and cognitive screening parameters. All relevant citations are appropriately included and discussed.
2. **Interpretation**: Retinal amyloid count (RAC) in the superotemporal quadrant is increased in patients with the Montreal Cognitive Assessment (MOCA) score < 26. Furthermore, RAC inversely correlates with hippocampal volumes. Based on our new topographical sub-regional analysis, amyloid count in the proximal mid-periphery solely showed more significant increase in MCI/AD patients as compared with cognitively normal individuals and was associated with lower hippocampal volume.
3. **Future directions**: The manuscript generates new data on regional retinal amyloid burden in patients with mainly MCI and provides great incentive to conduct future larger retinal imaging studies to confirm these findings as well as assesses correlations with brain amyloidosis and neurodegeneration. The specificity of retinal amyloid in the proximal mid-periphery (PMP) of the superotemporal quadrant needs to be replicated and the potential vulnerability of this retinal region elucidates in cognitively impaired individuals. Finally, the specific cut-off for RAC that is predictive of cognitive and brain volumetric scores needs determination.

TABLE 1 Patients' demographic characteristics, brain volumetric and retinal imaging parameters, stratified by Clinical Dementia Rating (CDR) and Montreal Cognitive Assessment (MOCA)

Variable	CDR 0.5 (n = 13)	CDR 1 (n = 17)	CDR 2 (n = 4)	*P*	MOCA > 26 (n = 18)	MOCA ≤ 26 (n = 16)	*P*
Age(years) (mean ± SD)	63 ± 6.53	65.41 ± 6.61	70.50 ± 9.11	.17	63.50 ± 6.69	66.94 ± 7.16	.15
Range	54-75	51-74	64-84		51–75	57-84	
Sex (n)				.25			.09
Male (M)	M (4)	M (9)	M (3)		M (6)	M (10)	
Female (F)	F (9)	F (8)	F (1)		F (12)	F (6)	
Years of education (mean ± SD)	16.6 ± 2.06	16.82 ± 1.87	16.50 ± 3.41	.94	16.25 ± 2.51	17.11 ± 1.56	.23
Co-morbid sleep disorder (%)	30	23	50	.52	25	33	0.6
GDS (mean ± SD)	5.9 ± 4.7	5.87 ± 3.99	3.33 ± 1.52	.60	5.57 ± 4.25	5.66 ± 4.01	.95
PSQ (mean ± SD)	57.38 ± 23.84	44.2 ± 22.65	62.0 ± 11.31	.38	43.80 ± 24.58	58.70 ± 18.88	.14
HTN (%)	38	35	25	.11	31	38	.65
HLD (%)	61	35	50	.38	50	44	.75
DM (%)	0	17	0	.20	12	5	.49
ICV (cm^3) (mean ± SD)	1532 ± 163	1522 ± 136.6	1532 ± 148.9	.98	1567 ± 164.2	1473 ± 94.92	.1
HV (cm^3) (mean ± SD)	7.50 ± 0.55	7.59 ± 0.82	5.93 ± 0.88	.004	7.64 ± 0.71	6.94 ± 0.93	.053
ILVV (cm^3) (mean ± SD)	1.67 ± 1.05	1.55 ± 0.60	4.09 ± 2.60	.006	1.45 ± 0.53	2.21 ± 1.75	.13
Total RA count (mean ± SD)	307.2 ± 79.57	300.6 ± 83.11	434.8 ± 109.3	.023	300.9 ± 82.66	339.1 ± 101.6	.23
Total RA area (mean ± SD)	1364 ± 347.9	1361 ± 596.6	1896 ± 575.4	.164	1460 ± 491.5	1394 ± 568	.72
PP RA count (mean ± SD)	81.62 ± 36.92	114.6 ± 52.91	126.8 ± 62.63	.12	92.06 ± 40.01	106.1 ± 46.57	.30
PP RA area (mean ± SD)	476.1 ± 228.7	503.1 ± 363.1	776.4 ± 282.6	.18	406.4 ± 203.6	465.1 ± 275.9	.49
PMP RA count (mean ± SD)	114.9 ± 51.65	113.9 ± 46.18	187.8 ± 58.33	.031	98.35 ± 33.81	142.1 ± 56.53	.01
PMP RA area (mean ± SD)	476.1 ± 228.7	503.1 ± 363.1	776.4 ± 282.6	.23	389.2 ± 135	593.6 ± 274.4	.01
DMP RA count (mean ± SD)	110.7 ± 60.61	72.0 ± 28.65	120.3 ± 68.59	.056	84.0 ± 38.67	91.0 ± 46.63	.64
DMP RA area (mean ± SD)	517.6 ± 370	342.9 ± 205.9	472.6 ± 233.9	.24	365.7 ± 175.0	374.2 ± 176.6	.89

Abbreviations: DM, diabetes mellitus; DMP, distal mid-periphery; GDS, Geriatric Depression Scale; HLD, hyperlipidemia; HTN, arterial hypertension; HV, hippocampal volume; ICV, intracranial volume; ILVV, inferior lateral ventricle volume; n, number; PMP, proximal mid-periphery; PP, posterior pole; PSQ, Pittsburg Sleep Questionnaire; RA, retinal amyloid; SD, standard deviation.

2 | METHODS

2.1 | Participants

This prospective cohort study received approval from the Cedars-Sinai Institutional Review Board. We enrolled subjects older than 40 years who presented to our neurology clinic with subjective cognitive decline and were interested in pursuing retinal imaging after signing an informed consent. All subjects underwent a neurological examination and standard battery of neuropsychological tests with a certified licensed neuropsychologist (DS). Their demographic information (age, gender, race, number of years of education), history, and clinical parameters were collected (see Table 1).

2.2 | Brain imaging

Subjects completed a standard-of-care 3 Tesla non-contrast structural brain magnetic resonance imaging (MRI). Automated NeuroQuant software was used for brain volumetric analysis[31] and the following parameters were collected: total intracranial volume (ICV) (cm^3), hippocampal volume (HV) (cm^3), and inferior lateral ventricle volume (ILVV) (cm^3).

2.3 | Retinal amyloid imaging

The study included a 4-day curcumin loading protocol. This was modified from the previously reported 10-day protocol, since the study showed that near-maximum red blood cell concentration of curcumin was measured after 4 days.[13] Each subject was provided with four packages of unencapsulated Longvida curcumin powder (20 grams each), four bottles of Ensure liquid nutritional shake, and four soft gels of vitamin E of 400 IU. The Longvida curcumin is specifically intended to increase curcumin bioavailability without co-ingestion of a glucuronidation inhibitor.[32] Subjects were instructed to take one package of curcumin mixed with the Ensure and one gel of 400 IU vitamin E once per day on an empty stomach, and 1 hour before breakfast. The vitamin E was used to further enhance bioavailability, augmenting the antioxidant used in the Longvida formulation to stabilize and to recycle curcumin and to prevent it from becoming a pro-oxidant in the body. Retinal imaging was performed several hours after the last curcumin mixture intake (day 4). After ocular dilation, a confocal scanning ophthalmoscope (Retia, CenterVue SpA) was used to obtain retinal images using blue light for excitation of curcumin emission to obtain images of the retina. The camera utilizes an illumination LED at 452 nanometers (nm) and uses a barrier filter to collect fluorescent emissions greater than or equal to 500 nm. The camera field of view is 60 degrees (H) x 55° (V), and the nominal optical resolution on the retina is 17 μm. At least 18 images of the superior retina were taken for each eye, six images at each of the three different focal planes (autofocus and ± 2 machine diopters) to accommodate focus variability and eye curvature. The superior retinal field is centered horizontally on the fovea and vertically 20 degrees above the fovea. The set of retinal images was processed using an investigational automated retinal fluorescence measurement software system (NeuroVision Imaging, Inc.). The software was fully automated, blinded to the operator, and functioned as follows: image sets for each eye were imported into the software and were algorithmically screened for image quality (including focus, contrast, variation in illumination, eye motion, obstruction, and proper fixation), and the software selected the eight highest quality images for further processing. These eight images were aligned and combined to reduce noise and further processed to reduce background variability and to maximize dynamic range. A common region of interest (ROI) was applied with a field of view of 50 degrees positioned on the image center, using fovea and optic nerve head centers as reference points to correct for eye rotation, with a zone around the fovea and optic nerve head masked. Pixels within the ROI manifest in a probability density function histogram that was mathematically characterized, and pixels that were abnormally intense compared to the retinal background structure were segmented and quantified. The repeatability coefficient of variation was found to be 8.7% for pixel count, and 11.6% for spot count, using a separately collected data set of 25 subject eyes, three repeat measures each on three machine-operator pairs. The ROI was further divided into three subregions: posterior pole (PP), proximal mid-periphery (PMP), and distal mid-periphery (DMP) (Figure 1). Retinal amyloid count (RAC) and total area were further quantified in the target ROI and the three subregions using NIH ImageJ software. The experiments conducting the image processing and quantifications were blinded to the patients' clinical characteristics.

2.4 | Assessments

The primary measures were differences in RAC or area in the three subregions of the superotemporal retina in subjects with Montreal Cognitive Assessment (MOCA) scores ≤26 (compared to scores >26) and correlation with HV. Secondary measures were differences in amyloid count or area in the three subregions of the supero-temporal retina according to Clinical Dementia Rating (CDR) scores 0.5, 1.0, and 2.0, as well as diagnostic groups, and correlation with HV.

2.5 | Statistical analysis

Descriptive statistics were calculated for patient demographics and clinical characteristics. Data are expressed as mean ± standard deviation unless otherwise stated. Groups were stratified based upon CDR and MOCA scores. MOCA scores of ≤26 were considered indicative of cognitive impairment, whereas score >26 indicate normal cognitive function.[33] CDR was stratified in three levels, with 0.5 indicating questionable dementia, one indicating mild cognitive impairment (MCI), and two indicating moderate cognitive impairment.[34] Group differences between continuous variables were evaluated using Student *t* test, while nominal qualitative variables were assessed using a chi-square test. Group differences between the three levels of CDR were assessed using one-way analysis of variance (ANOVA). Univariate associations between variables were assessed with Pearson correlation (r correlation coefficient). Cohen's d coefficient was used to assess the effect size. All statistical analyses were performed using GraphPad Prism 8.3. (GraphPad Software) with two-sided tests and a significance level of < 0.05.

2.6 | Patient population

The cohort included 18 female (52.94%) and 16 male (47.05%) patients. The mean age was 65 ± 7.03 (range 51 to 84) years. Most of the population (97.05%) was Caucasian, with only one subject being African American. Based on their neuropsychological reports, 8 subjects had normal cognitive scores, 22 had amnestic MCI, three had probable AD,

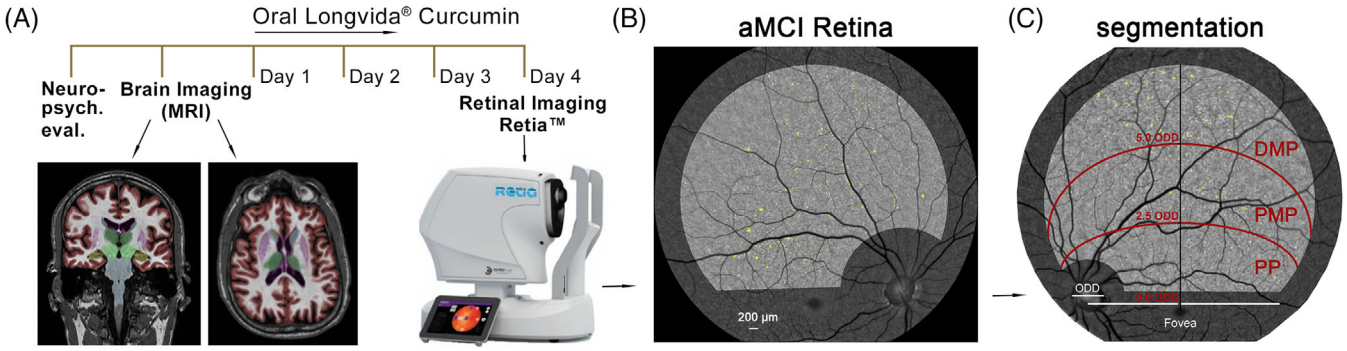

FIGURE 1 Illustration of the study timeline and topographical segmentation methodology for retinal amyloid analysis. Study timeline (A). Representative post-processed image of the retinal superotemporal quadrant from a subject with amnestic mild cognitive impairment (B) Illustration of the region of interest from the retinal supero-temporal quadrant and its predefined divisions, that were used for the quantification of the retinal amyloid plaque burden (C) aMCI, amnestic mild cognitive impairment (MCI); DMP, distal mid-periphery; ODD, optic disc diameter; PMP, proximal mid-periphery; PP, posterior pole

and one had possible frontotemporal dementia. The median MOCA score was 27 (range 4 to 30). From the total of 34 subjects, 13 subjects had a CDR classification of 0.5 (32.23%), 17 had a CDR of 1 (50%), and 4 subjects had a CDR of 2 (11.76%). Patient demographics and comorbid conditions were not different when compared according to MOCA or CDR scores, and HV and ILVV were significantly different between the three levels of CDR score (Table 1).

3 | RESULTS

All retinal amyloid parameters showed a significant correlation between the right and the left eyes (Pearson r = 0.63 [P = .002] for total RAC and Pearson r = 0.67 [P = .0003] for total RA area in the ST quadrant) and were similar in male and female patients [P > .05 for all comparisons (not shown)]. Study timeline and topographical segmentation of retinal amyloid images are described in Figure 1. Representative retinal images from subjects with different MOCA (female and male) and CDR values are illustrated in Figures 2A-D and 3A, respectively. The left eye was chosen arbitrarily for the comparative and correlation analyses. When compared for retinal amyloid parameters, the sub-regional analysis suggested that the PMP region of the superotemporal retina was preferentially predictive of severe cognitive deficits, where amyloid count and area were significantly higher in subjects with greater CDR and lower MOCA score (Table 1, Figure 2E-F, and Figure 3C). Patients with lower MOCA had lower total ICV (P = .09) and HV (P = .05) (Figure 2G-H). In addition, the total RAC was significantly different between the three CDR groups (Figure 3B; P = 0.023). Age was correlated significantly with ILVV (r = 0.48, P = .01), but not with HV or ICV. Age was not significantly correlated with any of the retinal parameters, although PMP amyloid area did approach significance (r = 0.33, P = .052). Both MOCA and CDR correlated with HV and ILVV (P < .05). The CDR score significantly correlated with total RAC (r = 0.38, P = .02) and PMP amyloid count (r = 0.37, P = .02). The total RAC significantly correlated with HV (Figure 2I; r = - 0.39, P = .04), whereas its correlation with ICV reached near statistical significance (P = .06). On subregion analysis, only the RAC in the PMP correlated with HV (Figure 2J; r = − 0.41, P = .03). When compared to individuals with normal cognition, the group of subjects with amnestic MCI and probable AD had significantly higher RAC in the PP and PMP subregions (Figure 3D and 3E; P = .036 and P = .042, respectively), with a large effect size (Cohen d = 0.83). Large effect sizes were also demonstrated by the comparisons between RAC and respective area, which were significantly greater in patients with MOCA ≤26 compared to MOCA >26 (Cohen d = 0.83 and 0.81, respectively). The RAC and area were found to be highly correlated (Pearson r = 0.74 (P < .001) for the association between total RAC and total retinal amyloid area; Pearson r = 0.84 (P < .001) for the association between PMP and PMP retinal amyloid area).

4 | DISCUSSION

Our study exploring RAI features with Retia confocal digital imaging device in a cohort of patients with cognitive decline is the first comprehensive study quantitatively evaluating subregional distribution of the superotemporal retinal amyloid burden in patients with mostly early cognitive impairment, and assessing the relationship with cognitive scores and brain volumes. Because the retinal amyloid quantification was blinded to the clinical and brain imaging parameters, the findings are not related to any bias. Furthermore, subjects were balanced for sex and age as confounders in experimental groups; hence, we believe the observed elevated retinal amyloid burden is specific to AD pathological changes. As the effects were independent of right vs left eye, but amyloid PET imaging was not performed, it remains unclear if differential amyloid left and right eye predict asymmetric burden, as is commonly leftward in primary progressive aphasia and rightward with visual spatial impairment.[35] The significant association between retinal amyloid burden, especially in the PMP topographical region, paired with significantly lower HV and poor cognitive scores, suggests the possibility for early detection of neurodegeneration through a retinal scan.

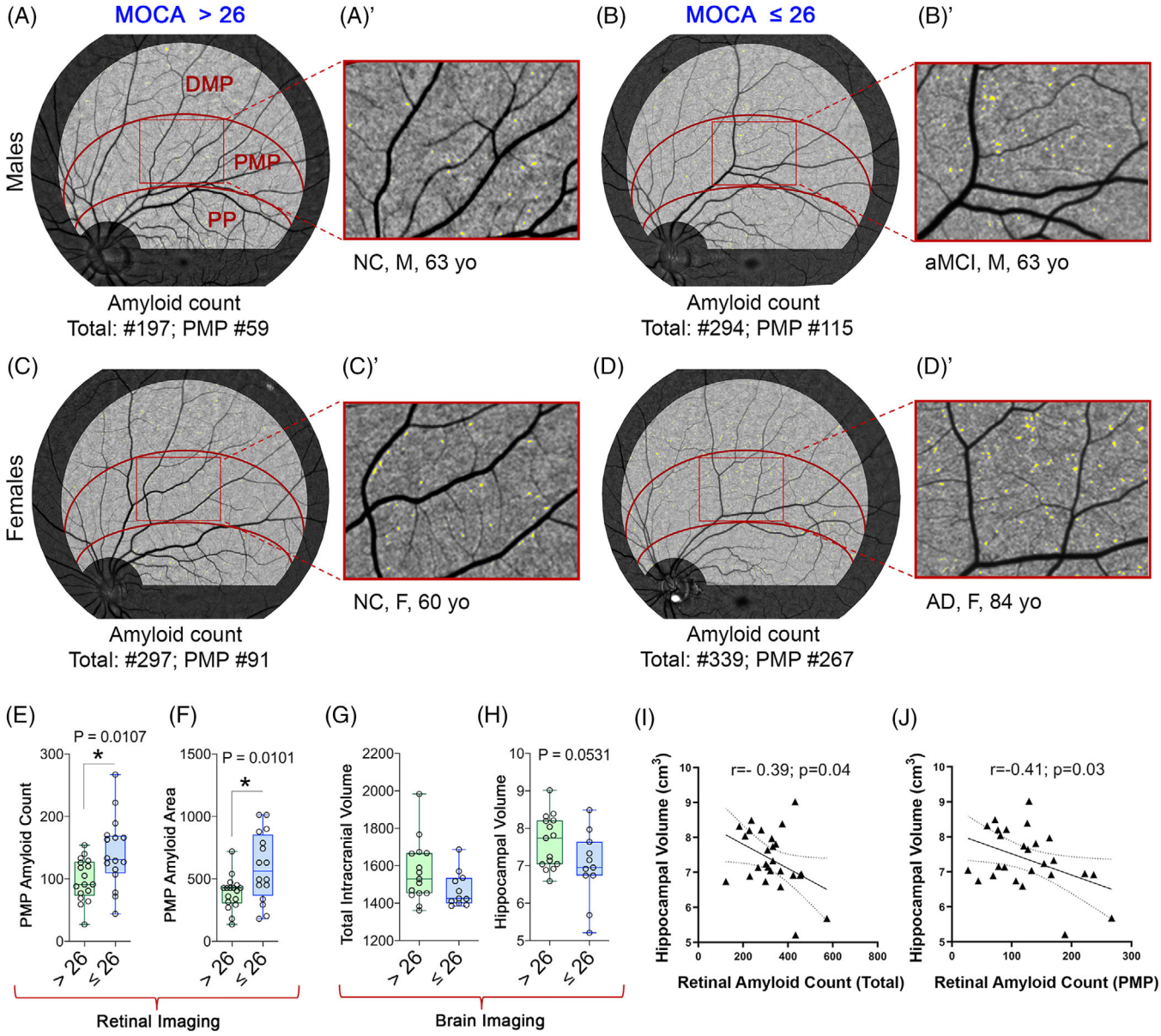

FIGURE 2 Retinal amyloid plaque scores per topographical regions for individuals stratified by the Montreal Cognitive Assessment (MOCA) score of 26. Representative fluorescent fundus images (A-D'). Graphs illustrating the differences in the proximal mid-periphery (PMP) amyloid count (E) and area (F), and total intracranial volume (G) and hippocampal volume (H) when stratified by MOCA score. Graphs illustrating the correlations between the hippocampal volume and total (I) and proximal mid-periphery (PMP) (J) retinal amyloid count. DMP, distal mid-periphery; PP, posterior pole. Whiskers bar graphs are showing individual data points as well as mean and deviation (* $P < .05$ by two-tailed paired Student t test)

The retinas derived from AD patients are hallmarked by an array of pathologies that mirror the disease in the brain, characterized not only by Aβ deposits, but also phosphorylated tau, vasculopathy, inflammation, and neurodegeneration.[7–16,32,36,37] We translated the RAI in clinical studies as a safe and non-invasive tool for retinal curcumin-labeled Aβ plaque imaging, with the potential of early detection of a pathological biomarker of AD.[7,13] Although curcumin, like other anti-Aβ compounds including the FDA-approved PiB compound, can bind to other misfolded proteins such as alpha-synuclein and tau, it was shown to have a markedly higher affinity as compared with the other compounds to Aβ fibrils, plaques, and oligomers, and especially to the 1-42 aa long alloform A$\beta_{1\text{-}42}$.[38–44] The ability to image, quantify, and/or label cerebral and retinal Aβ deposits with high specificity using curcumin, administered either orally or intravenously, was previously demonstrated.[7,9,13,28] Here, we demonstrated that our curcumin-enhanced retinal fluorescence amyloid imaging approach can be further translated into a systematic imaging protocol with fully automated fluorescence quantification software, as described in the methods section that now allows repeatable measurement for further clinical studies.

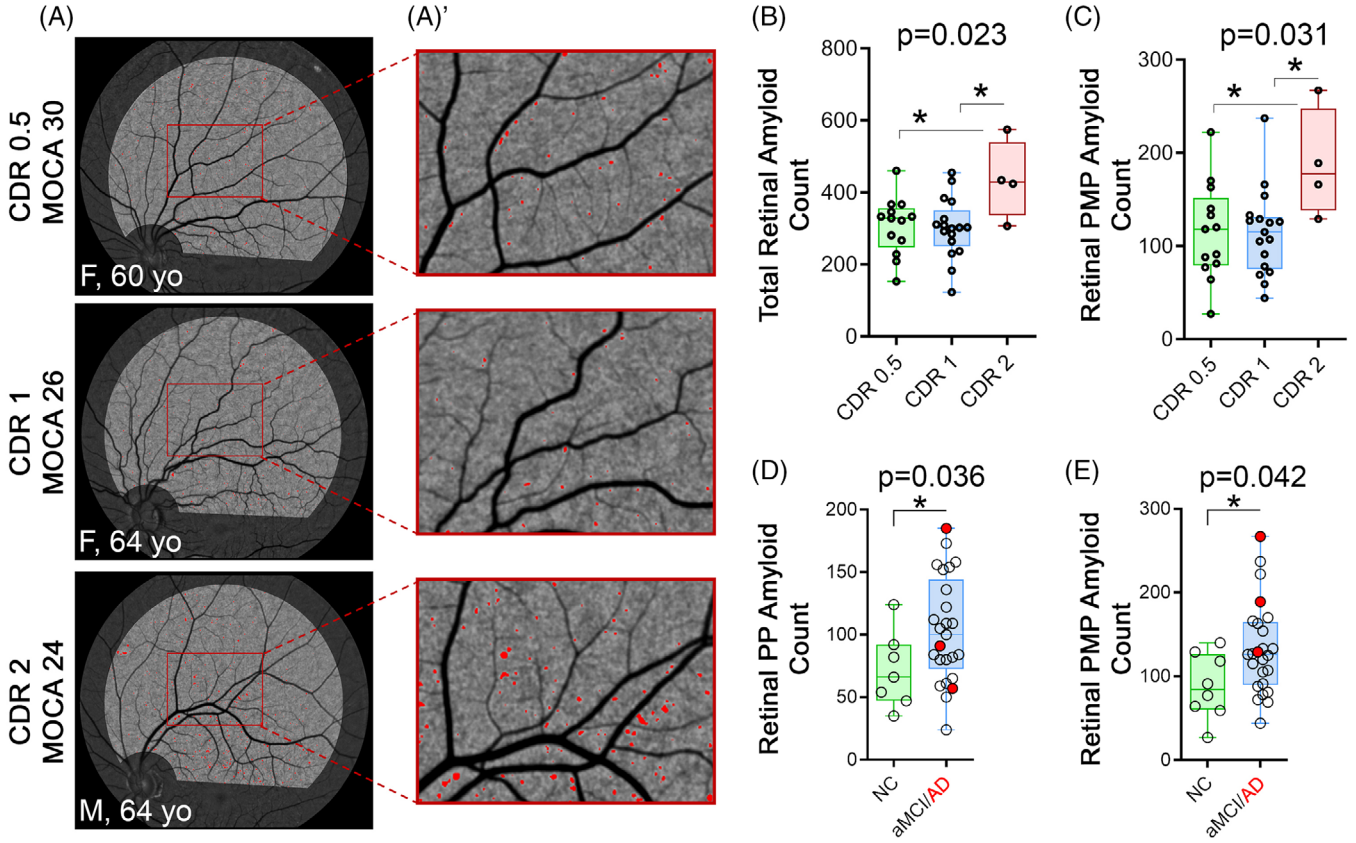

FIGURE 3 Retinal amyloid plaque scores in total and PMP region for individuals stratified by Clinical Dementia Rating (CDR) scores and clinical diagnosis. Representative fundus images in three patients of similar age group, demonstrating increased retinal amyloid count with higher CDR (A-A'). Graphs illustrating the differences between total (B) and proximal mid-periphery (PMP) (C) RAC stratified by CDR. Graphs illustrating the differences in the RAC in the posterior pole (PP) (D) and PMP (E), when stratified by diagnostic groups. Alzheimer's disease (AD), probable AD; aMCI, amnestic MCI; MOCA, Montreal Cognitive Assessment; NC, normal cognition. Whiskers bar graphs are showing individual data points as well as mean and deviation (* $P < .05$ by two-tailed paired Student *t*-test)

Drusenoid structures can also be found in the peripheral retina in cognitively impaired individuals.[45] Anderson et al.[46] showed that drusen contains nonfibrillar Aβ structures; hence it is possible that curcumin binds to drusenoid structures as well. A drusenoid structure, which may contain Aβ, can be potentially distinguished from a retinal amyloid plaque spatially and morphologically by using spectral domain optical coherence tomography.[45] Subsequent studies should assess the value of multimodal retinal imaging for specific delineation of the Aβ structures.

In this cohort study, total and PMP RAC in the superotemporal quadrant correlated significantly with HV and CDR, supporting a possible association between RAC and AD stage. When stratified based on clinical diagnoses, patients with amnestic MCI and probable AD showed significantly greater amyloid accumulation in the PMP and the PP regions, with a large effect size. Note that this increase in retinal amyloid burden remained significant even after the three probable AD patients were removed and the comparison was only with aMCI patients (not shown). However, when stratified according to MOCA (≤26 or >26), the PMP showed the most significant differences in amyloid count and area that were higher with more advanced cognitive impairment and lower HV. Although older patients tended to have more amyloid accumulation solely in the PMP area as well, there were no significant differences in the mean age between cognitive groups, so aging is insufficient to explain the differences. Furthermore, the total and PMP RAC and area were highly correlated but not identical due to diverse plaque size, which affects the amyloid area. In the PMP region though, both RAC and area yielded significantly higher values for patients with MOCA of ≤26 vs those with MOCA >26, with large effect sizes of 0.83 and 0.81, respectively. This suggests that future studies should focus on the PMP region of the superotemporal quadrant, which may be a more sensitive and specific indicator of the cognitive status. Our findings support prior observations that there is an increased Aβ deposition in the superotemporal quadrant in retinal flat mounts derived from neuropathologically confirmed AD patients.[7,12,13] These findings are also in agreement with previous studies pointing to this retinal region for increased degeneration, atrophy, and vascular pathology in MCI or AD.[12,17,30]

The role of vascular dysregulation, neurovascular unit impairment, and blood-brain barrier (BBB) disruption in AD is increasingly recognized,[47,48] with BBB pericyte injury being found as a predictor of apolipoprotein E (*APOE*) ε4–associated cognitive decline.[49] Shi et al identified early and progressive pericyte marker platelet-derived

growth factor receptor-β (PDGFRβ) deficiency and pericyte loss in post-mortem retinal vasculature derived from MCI and AD patients. These findings were also associated with retinal vascular amyloidosis and AD pathology in the brain.[17] Aβ accumulation inside retinal pericytes in AD and pericyte degeneration in the retina mirrored prominent features of brain AD pathology.[17,50] In this study, most subjects had vascular risk factors. Their retinal vasculature pathological changes are likely related to the retinal amyloid burden, as nowadays we have a better understanding of the relationship between vascular disease and AD. Future studies may consider addressing RAI in patients without any vascular risk factors; however, this current approach is more likely to preserve generalizability and clinical applicability.

The reason that PMP seems to be more vulnerable to AD pathology including Aβ accumulation remains unknown. It is possible that this phenomenon is rooted in the physiological structure of this retinal region, making it increasingly prone to disease processes or connecting it to brain pathology. Of interest, this temporal PMP retinal region is considered clinically to be most vulnerable to glaucoma-related neuronal damage,[51] and retinal nerve fiber layer shows disproportionate thinning in AD patients.[52] It is also conceivable that technically our current Retia ophthalmic device generated lower or inconsistent image quality/resolution for DMP regions, which impacted data reliability. The PMP region is consistently in better focus and with higher image quality, so therefore possibly better able to discern subtle amyloid plaque. Future studies are warranted to further investigate and validate these questions.

The significant relationship between retinal PMP amyloid count and HV suggests that quantitative RAI may be a useful biomarker to predict the progression to AD. On the same line, a recent biochemical study demonstrated that the levels of retinal high-molecular weight Aβ40 and Aβ42 significantly correlated with their corresponding levels in the hippocampus as well as with brain neurofibrillary tangle and Aβ scores.[16] The ability to screen for early CNS amyloidosis using a retinal scan in asymptomatic or early symptomatic patients is very relevant. Finding individuals with AD pathology before the clinical manifestation of dementia may open a window of opportunity for early intervention, as disease-modifying therapies are more likely to be effective if applied in early disease stages before neurodegeneration develops.[53] Although higher brain Aβ load assessed by amyloid PET in CN individuals with subjective cognitive impairment is associated with faster rates of cognitive decline,[54] the relationship between amyloid burden and cognition is complex and stage dependent. Nevertheless, it is an important outcome in clinical trials. Therefore, validation of PET amyloid association with retinal PMP amyloid would allow an economical biomarker for longitudinal studies. Furthermore, other accepted biomarkers (CSF low Aβ and high tau) are recognized as predictors of progression to AD,[55] but require invasive collection of CSF, so it is important to determine the relationship between these CSF biomarkers and retinal PMP plaques.

Although our study sample size was comparative to similar retinal imaging studies,[22] the data need to be validated with larger sample sizes. Our population was the majority Caucasian; therefore, our findings may not be generalized to other ethnicities. Group stratification and data analysis were based on cognitive screening measures, and only four subjects had a CDR of 2. Given the heterogeneity in sample size across study groups, and low numbers of probable AD patients, further confirmation of these interesting preliminary findings will be necessary in the future. Additional analyses exploring retinal amyloid burden with genetic markup and more robust neuropsychological instruments may provide greater specificity between retinal markers and cognitive performance indicators.

5 | CONCLUSION

Our study provides evidence that RAI is feasible using the Retia device with the automated retinal fluorescence measurement software, and able to detect increased retinal amyloid burden, especially in the PMP region, in patients with MCI. Future studies should assess the diagnostic and screening value of RAI, focusing on retinal amyloid correlation with brain Aβ and other markers of neurodegeneration.

CONFLICT OF INTEREST

Keith L. Black, Steven Verdooner, Yosef Koronyo, and Maya Koronyo-Hamaoui are co-founding members of NeuroVision Imaging Inc. Keith L. Black, Steven Verdooner, and Czeszynski Alan D are in leading roles in NeuroVision Imaging Inc. Keith L. Black, Steven Verdooner, Yosef Koronyo, and Maya Koronyo-Hamaoui are co-inventors of US patents related to retinal imaging and Alzheimer's disease. Sally Frautschy is co-inventor on US patent US9192644B2 for a curcumin formulation and is a co-founding member of Optimized Curcumin Longvida. Other authors declare no conflict.

REFERENCES

1. van de Kreeke JA, Nguyen HT, Konijnenberg E, et al. Optical coherence tomography angiography in preclinical Alzheimer's disease. *Br J Ophthalmol*. 2020;104(2):157-161.
2. Jack CR, Jr, Bennett DA, Blennow K, et al. NIA-AA research framework: toward a biological definition of Alzheimer's disease. *Alzheimers Dement*. 2018;14(4):535-562.
3. Elmaleh DR, Farlow MR, Conti PS, Tompkins RG, Kundakovic L, Tanzi RE. Developing effective Alzheimer's disease therapies: clinical experience and future directions. *J Alzheimers Dis*. 2019;71(3):715-732.
4. Tang W, Huang Q, Wang Y, Wang ZY, Yao YY. Assessment of CSF Abeta42 as an aid to discriminating Alzheimer's disease from other dementias and mild cognitive impairment: a meta-analysis of 50 studies. *J Neurol Sci*. 2014;345(1-2):26-36.
5. Seo SW, Ayakta N, Grinberg LT, et al. Regional correlations between [(11)C]PIB PET and post-mortem burden of amyloid-beta pathology in a diverse neuropathological cohort. *Neuroimage Clin*. 2017;13:130-137.
6. Blennow K, Mattsson N, Scholl M, Hansson O, Zetterberg H. Amyloid biomarkers in Alzheimer's disease. *Trends Pharmacol Sci*. 2015;36(5):297-309.
7. Koronyo-Hamaoui M, Koronyo Y, Ljubimov AV, et al. Identification of amyloid plaques in retinas from Alzheimer's patients and noninvasive in vivo optical imaging of retinal plaques in a mouse model. *Neuroimage*. 2011;54(Suppl 1):S204-S217.
8. Alexandrov PN, Pogue A, Bhattacharjee S, Lukiw WJ. Retinal amyloid peptides and complement factor H in transgenic models of Alzheimer's disease. *Neuroreport*. 2011;22(12):623-627.

9. Koronyo Y, Salumbides BC, Black KL, Koronyo-Hamaoui M. Alzheimer's disease in the retina: imaging retinal abeta plaques for early diagnosis and therapy assessment. *Neurodegener Dis*. 2012; 10(1-4):285-293.
10. Tsai Y, Lu B, Ljubimov AV, et al. Ocular changes in TgF344-AD rat model of Alzheimer's disease. *Invest Ophthalmol Vis Sci*. 2014;55(1):523-534.
11. Hart NJ, Koronyo Y, Black KL, Koronyo-Hamaoui M. Ocular indicators of Alzheimer's: exploring disease in the retina. *Acta Neuropathol*. 2016;132(6):767-787.
12. La Morgia C, Ross-Cisneros FN, Koronyo Y, et al. Melanopsin retinal ganglion cell loss in Alzheimer disease. *Ann Neurol*. 2016;79(1):90-109.
13. Koronyo Y, Biggs D, Barron E, et al. Retinal amyloid pathology and proof-of-concept imaging trial in Alzheimer's disease. *JCI Insight*. 2017;2(16):e93621.
14. den Haan J, Morrema THJ, Verbraak FD, et al. Amyloid-beta and phosphorylated tau in post-mortem Alzheimer's disease retinas. *Acta Neuropathol Commun*. 2018;6(1):147.
15. Grimaldi A, Pediconi N, Oieni F, et al. Neuroinflammatory processes, A1 astrocyte activation and protein aggregation in the retina of Alzheimer's disease patients, possible biomarkers for early diagnosis. *Front Neurosci*. 2019;13:925.
16. Schultz N, Byman E, Netherlands Brain B, Wennstrom M. Levels of retinal amyloid-beta correlate with levels of retinal IAPP and hippocampal amyloid-beta in neuropathologically evaluated individuals. *J Alzheimers Dis*. 2020;73(3):1201-1209.
17. Shi H, Koronyo Y, Rentsendorj A, et al. Identification of early pericyte loss and vascular amyloidosis in Alzheimer's disease retina. *Acta Neuropathol*. 2020;139(5):813-836.
18. Habiba U, Merlin S, Lim JKH, et al. Age-Specific retinal and cerebral immunodetection of amyloid-β plaques and oligomers in a rodent model of Alzheimer's disease. *J Alzheimer's Dis*. 2020;76(3):1135-1150.
19. Du LY, Chang LY, Ardiles AO, et al. Alzheimer's disease-related protein expression in the retina of octodon degus. *PLoS One*. 2015;10(8):e0135499.
20. More SS, Beach JM, McClelland C, Mokhtarzadeh A, Vince R. In vivo assessment of retinal biomarkers by hyperspectral imaging: early detection of Alzheimer's disease. *ACS Chem Neurosci*. 2019;10(11):4492-4501.
21. Latasiewicz M, Sala-Puigdollers A, Gonzalez-Ventosa A, Milla E, Adan Civera A. Multimodal retinal imaging of familial amyloid polyneuropathy. *Ophthalmic Genet*. 2019;40(5):407-420.
22. Hadoux X, Hui F, Lim JKH, et al. Non-invasive in vivo hyperspectral imaging of the retina for potential biomarker use in Alzheimer's disease. *Nat Commun*. 2019;10(1):4227.
23. Sharafi SM, Sylvestre JP, Chevrefils C, et al. Vascular retinal biomarkers improves the detection of the likely cerebral amyloid status from hyperspectral retinal images. *Alzheimers Dement (N Y)*. 2019;5:610-617.
24. Yang F, Lim GP, Begum AN, et al. Curcumin inhibits formation of amyloid beta oligomers and fibrils, binds plaques, and reduces amyloid in vivo. *J Biol Chem*. 2005;280(7):5892-5901.
25. Begum AN, Jones MR, Lim GP, et al. Curcumin structure-function, bioavailability, and efficacy in models of neuroinflammation and Alzheimer's disease. *J Pharmacol Exp Ther*. 2008;326(1):196-208.
26. Kunwar A BA, Priyadarsini IK, Pandey R. Absorption and fluorescence studies of curcumin bound to liposome and living cells. *BARC Newsletter*. 2007:213-219.
27. Ringman JM, Frautschy SA, Teng E, et al. Oral curcumin for Alzheimer's disease: tolerability and efficacy in a 24-week randomized, double blind, placebo-controlled study. *Alzheimers Res Ther*. 2012;4(5):43.
28. Garcia-Alloza M, Borrelli LA, Rozkalne A, Hyman BT, Bacskai BJ. Curcumin labels amyloid pathology in vivo, disrupts existing plaques, and partially restores distorted neurites in an Alzheimer mouse model. *J Neurochem*. 2007;102(4):1095-1104.
29. Ran C, Xu X, Raymond SB, et al. Design, synthesis, and testing of difluoroboron-derivatized curcumins as near-infrared probes for in vivo detection of amyloid-beta deposits. *J Am Chem Soc*. 2009;131(42):15257-15261.
30. Asanad S, Ross-Cisneros FN, Nassisi M, Barron E, Karanjia R, Sadun AA. The retina in Alzheimer's disease: histomorphometric analysis of an ophthalmologic biomarker. *Invest Ophthalmol Vis Sci*. 2019;60(5):1491-1500.
31. Engedal K, Braekhus A, Andreassen OA, Nakstad PH. Diagnosis of dementia—automatic quantification of brain structures. *Tidsskr Nor Laegeforen*. 2012;132(15):1747-1751.
32. Doustar J, Torbati T, Black KL, Koronyo Y, Koronyo-Hamaoui M. Optical coherence tomography in Alzheimer's disease and other neurodegenerative diseases. *Front Neurol*. 2017;8:701.
33. Damian AM, Jacobson SA, Hentz JG, et al. The montreal cognitive assessment and the mini-mental state examination as screening instruments for cognitive impairment: item analyses and threshold scores. *Dement Geriatr Cogn Disord*. 2011;31(2):126-131.
34. Morris JC. The Clinical Dementia Rating (CDR): current version and scoring rules. *Neurology*. 1993;43(11):2412-2414.
35. Frings L, Hellwig S, Spehl TS, et al. Asymmetries of amyloid-beta burden and neuronal dysfunction are positively correlated in Alzheimer's disease. *Brain*. 2015;138(Pt 10):3089-3099.
36. Hampel H, Toschi N, Babiloni C, et al. Revolution of Alzheimer precision neurology. Passageway of systems biology and neurophysiology. *J Alzheimers Dis*. 2018;64(s1):S47-S105.
37. Dumitrascu OM, Qureshi TA. Retinal vascular imaging in vascular cognitive impairment: current and future perspectives. *J Exp Neurosci*. 2018;12:1179069518801291.
38. Yanagisawa D, Amatsubo T, Morikawa S, et al. In vivo detection of amyloid beta deposition using (1)(9)F magnetic resonance imaging with a (1)(9)F-containing curcumin derivative in a mouse model of Alzheimer's disease. *Neuroscience*. 2011;184:120-127.
39. Yanagisawa D, Shirai N, Amatsubo T, et al. Relationship between the tautomeric structures of curcumin derivatives and their Abeta-binding activities in the context of therapies for Alzheimer's disease. *Biomaterials*. 2010;31(14):4179-4185.
40. Airoldi C, Zona C, Sironi E, et al. Curcumin derivatives as new ligands of Abeta peptides. *J Biotechnol*. 2011;156(4):317-324.
41. Mutsuga M, Chambers JK, Uchida K, et al. Binding of curcumin to senile plaques and cerebral amyloid angiopathy in the aged brain of various animals and to neurofibrillary tangles in Alzheimer's brain. *J Vet Med Sci*. 2012;74(1):51-57.
42. Kumaraswamy P, Sethuraman S, Krishnan UM. Mechanistic insights of curcumin interactions with the core-recognition motif of beta-amyloid peptide. *J Agric Food Chem*. 2013;61(13):3278-3285.
43. Masuda Y, Fukuchi M, Yatagawa T, et al. Solid-state NMR analysis of interaction sites of curcumin and 42-residue amyloid beta-protein fibrils. *Bioorg Med Chem*. 2011;19(20):5967-5974.
44. Ryu EK, Choe YS, Lee KH, Choi Y, Kim BT. Curcumin and dehydrozingerone derivatives: synthesis, radiolabeling, and evaluation for beta-amyloid plaque imaging. *J Med Chem*. 2006;49(20):6111-6119.
45. Cabrera DeBuc D, Somfai GM, Arthur E, Kostic M, Oropesa S, Mendoza Santiesteban C. Investigating multimodal diagnostic eye biomarkers of cognitive impairment by measuring vascular and neurogenic changes in the retina. *Front Physiol*. 2018;9:1721.
46. Anderson DH, Talaga KC, Rivest AJ, Barron E, Hageman GS, Johnson LV. Characterization of beta amyloid assemblies in drusen: the deposits associated with aging and age-related macular degeneration. *Exp Eye Res*. 2004;78(2):243-256.
47. van de Haar HJ, Jansen JFA, van Osch MJP, et al. Neurovascular unit impairment in early Alzheimer's disease measured with magnetic resonance imaging. *Neurobiol Aging*. 2016;45:190-196.

48. Iturria-Medina Y, Sotero RC, Toussaint PJ, Mateos-Perez JM, Evans AC, Alzheimer's Disease Neuroimaging I. Early role of vascular dysregulation on late-onset Alzheimer's disease based on multifactorial data-driven analysis. *Nat Commun*. 2016;7:11934.
49. Montagne A, Nation DA, Sagare AP, et al. APOE4 leads to blood-brain barrier dysfunction predicting cognitive decline. *Nature*. 2020;581(7806):71-76.
50. Bell RD, Zlokovic BV. Neurovascular mechanisms and blood-brain barrier disorder in Alzheimer's disease. *Acta Neuropathol*. 2009;118(1):103-113.
51. Quigley HA, Addicks EM, Green WR. Optic nerve damage in human glaucoma optic nerve damage in human glaucoma. iii. Quantitative correlation of nerve fiber loss and visual field defect in glaucoma, ischemic neuropathy, papilledema, and toxic neuropathy. *Arch Ophthalmol*. 1982;100(1):135-146.
52. Jones-Odeh E, Hammond CJ. How strong is the relationship between glaucoma, the retinal nerve fibre layer, and neurodegenerative diseases such as Alzheimer's disease and multiple sclerosis? *Eye (Lond)*. 2015;29(10):1270-1284.
53. Briggs R, Kennelly SP, O'Neill D. Drug treatments in Alzheimer's disease. *Clin Med (Lond)*. 2016;16(3):247-253.
54. Timmers T, Ossenkoppele R, Verfaillie SCJ, et al. Amyloid PET and cognitive decline in cognitively normal individuals: the science project. *Neurobiol Aging*. 2019;79:50-58.
55. Devanarayan P, Devanarayan V, Llano DA, and for the Alzheimer's Disease Neuroimaging I. Identification of a simple and novel cut-point based cerebrospinal fluid and mri signature for predicting Alzheimer's disease progression that reinforces the 2018 NIA-AA research framework. *J Alzheimers Dis*. 2019;68(2):537-550.

How to cite this article: Dumitrascu OM, Lyden PD, Torbati T, et al. Sectoral segmentation of retinal amyloid imaging in subjects with cognitive decline. *Alzheimer's Dement*. 2020;12:e12109. https://doi.org/10.1002/dad2.12109